Study of $\alpha + d$ and $^3He + t$ Clustering in ^6Li with a Two-Mode, Finite-Range Analysis of the $^6Li(p, ^3He)^4He$ Reaction*

Michael F. Werby, M. B. Greenfield, K. W. Kemper, D. L. McShan, and Steve Edwards
Department of Physics, The Florida State University, Tallahassee, Florida 32306
(Received 7 February 1973)

The $^6Li(p, ^3He)^4He$ reaction was studied at incident proton energies of 12, 14, and 16 MeV. Detection of both the ^3He and ^4He particles in the lab defined angular distributions from about 10 to 170° c.m. The data taken as well as existing data at 8, 10, and 18.5 MeV were analyzed using a finite-range multi-interaction distorted-wave Born-approximation formalism to determine the importance of clustering in the ^6Li nucleus as well as the importance of various reaction mechanisms. Reduced widths of 0.69 for $\alpha + d$ in a relative s state, 0.04 for $\alpha + d$ in a relative d state, and 0.44 for $^3He + t$ in a relative s state provided fits to the data at 12, 14, 16, and 18.5 MeV.

I. INTRODUCTION

The ^6Li nucleus has frequently been described by the $\alpha + d$ cluster model. Such a description has accounted for many of the properties of that nucleus.[1] Because of the rather weak binding between the α and d clusters that form ^6Li, that description is thought to be energetically favored over other cluster configurations.[2] However, more recently some attention has been given to the $^3He + t$ description of ^6Li in which some authors[3,4] find evidence of significant $^3He + t$ clustering while others[5] do not. It is possible to have considerable $\alpha + d$ and $^3He + t$ clustering at the same time,[6] and the importance of both configurations may be examined by analyzing angular distributions of the $^6Li(p, ^3He)^4He$ reaction using a finite-range two-mode multi-interaction distorted-wave Born-approximation (DWBA) formalism.[7]

In such a two-mode formalism, exchange modes arise from the antisymmetrization of the total initial-state or final-state wave function. For the direct mode, the outgoing particle, ^3He, is made up of the bombarding particle p and a transferred particle (in this case, a deuteron). We write the process as follows

$$p + (^6Li = \alpha \oplus d) \rightarrow (^3He = d \oplus p) + ^4He\,. \quad (1)$$

For the exchange mode, the outgoing particle is emitted from the target nucleus, and the process appears as follows

$$p + (^6Li = ^3He \oplus t) \rightarrow ^3He + (\alpha = p \oplus t)\,. \quad (2)$$

In this paper, angular distributions of the reaction are analyzed using the finite-range multi-interaction computer code FANLU 2.[8] The importance of the various interactions is examined and spectroscopic factors of the two-cluster configurations are extracted from the data.

II. EXPERIMENT

Angular distributions were obtained for the $^6Li(p, ^3He)^4He$ reaction at proton energies of 12, 14, and 16 MeV. Detection of both exit channel nuclei at forward angles in the lab provided angular distributions from about 10 to 170° c.m. Targets were bombarded with the proton beam from the Florida State University super FN tandem accelerator.

Targets of 99.9% isotopically enriched ^6Li were prepared by slowly evaporating the enriched metal onto a thin Formvar backing a few hours before running. The targets were kept and transported in vacuum of less than 10^{-4} Torr to prevent atmospheric contamination and decomposition. Target thickness was measured and continuously monitored by observing elastically scattered protons with fixed geometry at 95° lab. Target thicknesses were typically 15 $\mu g/cm^2$, and no loss of Li was observed after 12 hours running time. Target nonuniformity was $\leq 10\%$ but contributed no experimental error since each data point was normalized to the elastic yield at 95°.

Detection and identification of ^3He and ^4He particles were facilitated by means of a Si surface-barrier telescope consisting of a 50-μm transmission counter and a 300-μm stopping counter. Collimation was provided such that the target frame and beam defining slits could not be viewed by the telescope and such that small-angle scattering from defining slits was negligible. The identification and resolution of ^3He and ^4He groups were such that errors in extracting peak areas were due solely to counting statistics. A typical energy spectrum is shown in Fig. 1. Statistics produced the only relative experimental errors, since the data were normalized to the elastic scattering yield from a fixed geometry counter. Error in the absolute normalization is based on

the error in determining the monitor counter solid angle 2%, beam current normalization 5%, error due to background subtraction from the elastic proton yield in the monitor counter 5%, and the reported experimental error in the measured elastic scattering cross section 4%.[9] These factors yield a total error in the absolute normalization of ~10%.

III. MULTI-INTERACTION FORMALISM

The multi-interaction exact finite-range two-mode DWBA formalism has been given elsewhere,[10] and we merely give those parts of the formalism that are necessary for understanding our analysis of the the ^{6}Li$(p,{}^3$He$)^4$He reaction. The total direct transition amplitude is

$$T^D = \langle f \mid V_{pd} + V_{p\alpha} - \overline{U}_{p^6\mathrm{Li}} \mid i \rangle , \tag{3}$$

where $|i\rangle$ and $\langle f|$ contain initial- and final-state distorted-wave information, V_{xy} designates the interaction between pairs of particles x and y and, $\overline{U}_{p^6\mathrm{Li}}$ generates the incident distorted waves. The exchange amplitude is:

$$T^E = \langle f \mid V_{pt} + V_{p^3\mathrm{He}} - \overline{U}_{p^6\mathrm{Li}} \mid i \rangle . \tag{4}$$

The complete transition amplitude is then:

$$T = N_D T^D + N_E T^E , \tag{5}$$

where N_D and N_E are statistical factors which give the number of direct and exchange amplitudes as determined by the number of exchangeable particles. The interaction V_{pd} is associated with light particle or direct pickup, $V_{p\alpha}$ is associated with direct or heavy particle knockout, V_{pt} is associated with exchange or heavy particle pickup, and $V_{p^3\mathrm{He}}$ with exchange or light particle knockout.

Both structure and scattering state information are contained in the quantities $|i\rangle$ and $\langle f|$. In the direct mode, the target ^{6}Li is expanded on a basis that includes the ground state of an α particle and that of a deuteron with relative motion $\phi_{\alpha d}$. The relative motion wave function $\phi_{\alpha d}$ is a mixture of $2s$ and $1d$ states to be discussed later.[11] The helion is expanded in a relative $1s$ state designated by ϕ_{dp}.

For the exchange mode, ^{6}Li is expanded on a basis that includes the ground state of a triton and ^{3}He in a relative $2s$ state, designated by $\phi_{^3\mathrm{He}t}$. The remaining relative motion state in the exchange mode is between a triton and a proton in a relative $1s$ state designated by ϕ_{pt}.

Since $\phi_{\alpha d}$ has both $2s$ and $1d$ components, it is possible to divide T^D into two components

$$T^D = T^D_{2s} + T^D_{1d} , \tag{6}$$

where the subscripts designate the contributions of the $2s$ and $1d$ components of the $\phi_{\alpha d}$ system to the total direct amplitude. This enables one to calculate the components of the transition amplitude associated with the distinct states of the $\alpha + d$ configuration.

It can be shown that[12]:

$$N^D T^D_{2s} = [\, S^{^6\mathrm{Li}}_{\alpha d}(2s)\, S^{^3\mathrm{He}}_{dp}(1s)]^{1/2}\, t^D_{2s} , \tag{7}$$

$$N^D T^D_{1d} = [\, S^{^6\mathrm{Li}}_{\alpha d}(1d)\, S^{^3\mathrm{He}}_{dp}(1s)]^{1/2}\, t^D_{1d} , \tag{8}$$

$$N^E T^E = [\, S^{^6\mathrm{Li}}_{^3\mathrm{He}t}(2s)\, S^{\alpha}_{pt}(1s)]^{1/2}\, t^E . \tag{9}$$

Here $S^z_{xy}(a)$ designates the spectroscopic factor of system z made up of clusters x and y in relative motion state a. The quantities t are transition amplitudes calculated from bound-state wave functions and reduced widths normalized to unity.

The square roots of the products of spectroscopic factors are taken to be the only adjustable parameters, and their values are determined by fitting the experimental angular distributions. The values of $S^{\alpha}_{pt}(1s)$ and $S^{^3\mathrm{He}}_{pd}(1s)$ have been determined elsewhere[13] and are 2.0 and 1.35, respectively. Thus, one can obtain the values of $S^{^6\mathrm{Li}}_{\alpha d}(2s)$, $S^{^6\mathrm{Li}}_{\alpha d}(1d)$, and $S^{^6\mathrm{Li}}_{^3\mathrm{He}t}(2s)$ in this analysis. It is to be pointed out that the relative signs of the adjustable factors are also impotant and are determined by the fitting method.

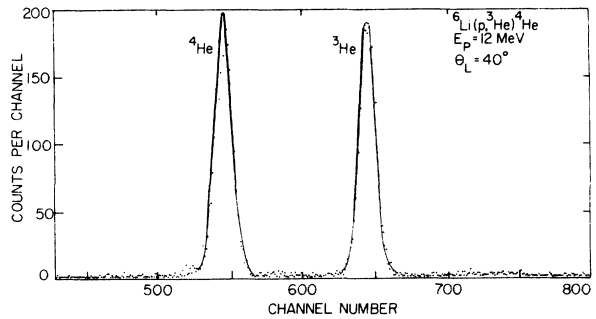

FIG. 1. Energy spectrum from the ^{6}Li$(p,{}^3$He$)^4$He reaction at 12 MeV.

IV. RELATIVE MOTION BOUND-STATE WAVE FUNCTIONS

A. $d+p$ Relative Motion Function

The radial part of the wave function describing the relative motion between a deuteron and a proton is taken as the overlap between ^{3}He and deuteron wave functions.

$$\phi_{dp} = \langle d | {}^3\mathrm{He} \rangle . \tag{10}$$

The ^{3}He wave function is assumed to have the Jastrow[14] form for the radial part, assuming only

the symmetric $1s$ state.

$$|^3\mathrm{He}\rangle = N\prod_{i=1} g(r_i), \tag{11}$$

where

$$g(r_i) = (e^{-ar_i} - e^{-br_i})/r_i^{1/2} \tag{12}$$

and N is a normalization constant. Here r_i is the separation between a pair of the three nucleons that make up ^{3}He, and a and b are the long and short range parameters. This form will yield the correct asymptotic shape of the wave function if a is chosen as follows[15]:

$$a = (mE_B/3)^{1/2}. \tag{13}$$

Here m is the mass of the nucleon and E_B is the difference between the binding energy of the helion and the effective binding energy of the deuteron. The parameter b was determined by adjusting its value to predict the experimental root-mean-square radius of the ^{3}He nucleus.[16] The resulting parameters are $a = 0.22$, $b = 2.10$. The overlap is then taken between the $1s$ component of the Gartenhaus solution for the deuteron wave function[17] and the ^{3}He wave function to yield ϕ_{dp}. The derived function ϕ_{dp} is only normalized to unity if ^{3}He is in a pure $1s$ relative $d+p$ state. This in fact is not expected, and the quantity

$$[\Theta^{^3\mathrm{He}}_{dp}]^2 = |\langle\phi_{dp}|\phi_{dp}\rangle|^2 \tag{14}$$

yields the probability of finding ^{3}He in a $d+p$ relative $1s$ state. This number is often assumed to be unity, but a calculation by this method predicts a value of 0.9 consistent with other results.[18] The spectroscopic factor is

$$S^{^3\mathrm{He}}_{dp} = \tfrac{3}{2}(\Theta^{^3\mathrm{He}}_{dp})^2. \tag{15}$$

The d state of the deuteron was not included in the derivation of $\phi^{^3\mathrm{He}}_{dp}$ since its contribution is expected to be small for the following reason. The wave function $\phi^{^3\mathrm{He}}_{dp}$ occurs as a product with V_{dp} for the pickup term. The short range nature of V_{dp} and the effect of the angular momentum barrier on the d state component of $\phi^{^3\mathrm{He}}_{dp}$ will result in little overlap between the two and thus will yield a small contribution from the direct pickup term. Since the direct knockout term is small for the $1s$ relative state component, it might be assumed that the d relative state component would also be small.

B. $\alpha+d$ Relative Motion Wave Function

The problem of obtaining the relative motion wave function between the α and d clusters making up ^{6}Li may be reduced to a three-body problem by treating α as fundamental and assuming the nucleons in the deuteron to interact with the α particle via an α-nucleon interaction and with themselves via a nucleon-nucleon potential. In order to formulate the problem mathematically, we set the wave function of ^{6}Li equal to the product of the deuteron wave function and the relative motion wave function $\phi_{\alpha d}$ between the centers of mass of the two clusters. In this method, one assumes that there is no distortion of the deuteron in the neighborhood of α, i.e. the no distortion approximation.[19]

One then substitutes this wave function for ^{6}Li into the Schrödinger equation and derives an equation which defines $\phi_{\alpha d}$ in terms of a Hamiltonian containing the potential

$$V_{\alpha d}(\rho) = \int\phi_d(r)[V_n(\vec{\rho}+\tfrac{1}{2}\vec{r}) + V_p(\vec{\rho}-\tfrac{1}{2}\vec{r})]\phi_d(r)d\vec{r}, \tag{16}$$

where $\vec{\rho}$ is the displacement vector between the centers of mass of α and d. The nucleon-α potentials V_p and V_n are of the form $V_0e^{-k^2x^2}$ with the Coulomb term added for V_p. The parameters V_0 and k are obtained from values used by Sack, Biedenharn, and Breit[20] in their analysis of elastic scattering between nucleons and α particles.

If the d component of the deuteron is included in the deuteron wave function, then the above potential will contain both a central and tensor term. The tensor term leads to a coupled set of linear differential equations and thereby predicts an s and d component for $\phi_{\alpha d}$ consistent with angular momentum and parity conservation for the system.

Rather than perform a lengthy calculation, we ignore the d component ϕ_d in deriving $V_{\alpha d}$ and obtain a central potential that contains a rather long tail. This method predicts a $2s$ $\phi_{\alpha d}$ state with a binding energy of 2.2 MeV, a value remarkably close to the 1.47-MeV value found experimentally. By reducing the value of V_0 obtained by Sack by less than 5%, it was possible to predict the actual experimental value. However, the $1d$ component was found to be slightly unbound, though one might expect binding to occur had the tensor term been included. In order to include the $1d$ state using this simplified method, the magnitude of V_0 was increased slightly to predict the correct binding energy of this system. The derived form factors are illustrated in Fig. 2.

C. Exchange Relative Motion Wave Functions

The relative motion wave function $\phi_{^3\mathrm{He}t}$ between ^{3}He and t is shown in Fig. 2. This wave function was obtained from a resonating group calculation performed by Thompson and Tang.[11] The remaining relative motion wave function for the $t+p$ sys-

tem was obtained by adjusting the geometric parameters and well depth of a Woods-Saxon potential to yield the experimental root-mean-square radius (charge radius).[16] Because of the very large separation energy between the two clusters ($E_{pt} \approx 20$ MeV), the relative motion wave function is constricted in space, and its shape is not sensitive to different methods of derivation; hence, we use the above simple potential well derivation.

Conservation of angular momentum and parity does not forbid $^3He + t$ to be in a $1d$ relative state. Including this state would have required the calculation of two additional transition amplitudes since the $1d$ state can overlap with both the $2s$ and $1d$ $\alpha + d$ relative states. The overlap between the two $1d$ states would require an extremely lengthy calculation because of the large number of radial integrals that occur from coupling the two $1d$ states. Characteristic cross sections from such overlaps tend to vary slowly with angle, especially in the backward direction, in contrast with the observed sharp backward peaking. Thus, the $1d$ relative state was not included in this analysis.

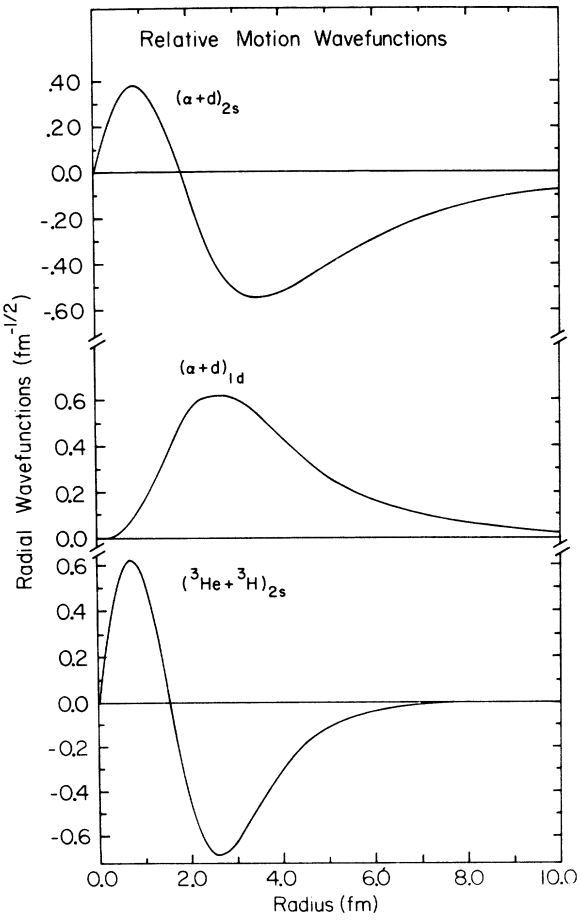

FIG. 2. Relative motion motion wave functions for $2s$ $\alpha + d$, $1d$ $\alpha + d$, and $2s$ $^3He + t$ cluster configurations of ^6Li.

TABLE I. Optical-model parameters.

Set	V_0	W_v	W_s	r_0	r_i	a_0	a_i
I. $p + {}^6Li$	57.6	0.0	6.6	1.15	1.15	0.6	0.5
II. $p + {}^6Li$	49.0	0.0	7.5	1.25	1.25	0.7	0.7
III. $^3He + \alpha$	100.0	0.0	8.5	1.35	1.35	0.6	0.6
IV. $^3He + \alpha$	80.0	6.0	0.0	1.50	1.50	0.6	0.6
V. $^3He + \alpha$	106.0	10.65	0.0	1.57	1.52	0.7	0.7
VI. $^3He + \alpha$	32.0	10.0	0.0	1.50	1.50	0.6	0.6

V. OPTICAL-MODEL PARAMETERS AND INTERACTION POTENTIALS

The optical-model parameters used in the calculations are listed in Table I. Set I was obtained by fitting elastic scattering data on $1p$-shell nuclei[21] while Set II was obtained by fitting polarization data of protons[22] on ^6Li. For the exit channel, Sets V[23] and VI[24] were obtained by fitting elastic scattering data at energies somewhat lower than required for the exit channel. The real parts of the potential Sets III and IV were obtained from potentials that bind $^3He + \alpha$ to form ^7Be with the appropriate binding energy.[13] The imaginary parts were added to account for absorption of particles into nonelastic channels.

The above parameter sets were used in a preliminary calculation that included only the $2s$ relative states of the $\alpha + d$ and $^3He + t$ systems. Qualitatively, shapes of the predicted cross sections were insensitive to the parameter sets. However, the magnitudes of the calculated cross sections and the resulting spectroscopic factors varied somewhat with extreme choices of exit channel sets (Sets V and VI). There was little effect when Sets I, II, III, and IV were interchanged. The maximum effect occurred in the exchange mode which amounted to a difference of not more than 20% in magnitude of the extracted spectroscopic factor. The parameters were not allowed to vary as a function of energy except for Set I which was

TABLE II. Interaction potentials.

Interaction	V_0 (MeV)	r_0 (fm)	a_0 (fm)
V_{pd}	39.5	1.59	0.600
$V_{p\alpha}$	45.0	1.40	0.435
$V_{p\,^3He}$	61.4	1.39	0.400
V_{pt}	61.4	1.39	0.400

varied according to the prescription proposed by Watson.[21] Only Sets I and III were used in all final calculations because of the rather large computer time needed for each calculation.

All interaction potentials were of the Woods-Saxon form, and their parameters are listed in Table II. The potentials V_{pd} and V_{pt} were obtained by adjusting the well depths and geometries so that the $p+d$ and $p+t$ bound systems yielded the experimental binding energies and root-mean-square radii for ^{3}He and α, respectively.[16] The potential $V_{p^3\mathrm{He}}$ was set equal to V_{pt}, and $V_{p\alpha}$ was obtained from the real part of a potential that described the elastic scattering of protons by α particles.[25]

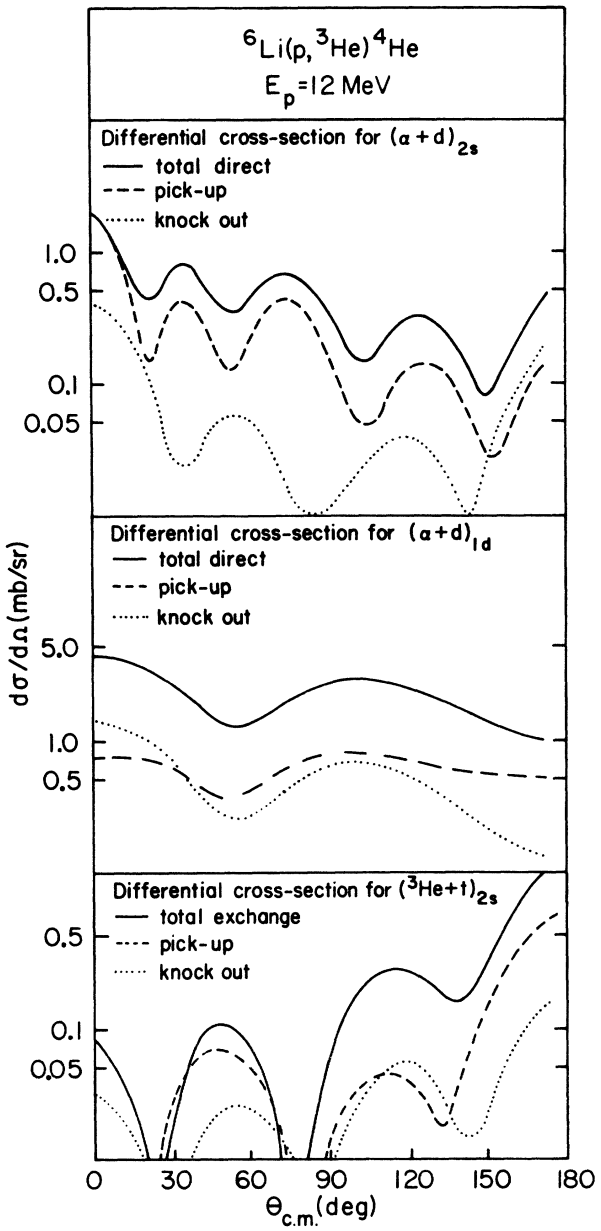

FIG. 3. Calculated angular distribution of differential cross sections for the ^{6}Li$(p,^3$He$)^4$He reaction at 12 MeV.

VI. EXTRACTION OF SPECTROSCOPIC FACTORS

The exact finite-range two-mode multi-interaction formalism discussed above was used to analyze data taken here as well as data taken by In Gun Han[26] at 8 and 10 MeV and by Likely and Brady[27] at 18.5 MeV. Figure 3 illustrates the shapes and relative importance of the various components that make up the total cross sections for the reaction at 12 MeV. It is apparent from the figure that contributions to the cross section from the relative motion wave functions $\phi_{\alpha d}$ and $\phi_{^3\mathrm{He}t}$ have distinguishing characteristic shapes which enables one to extract the spectroscopic factors unambiguously. In this study, the spectroscopic factors $S^{^6\mathrm{Li}}_{\alpha d}(2s)$, $S^{^6\mathrm{Li}}_{\alpha d}(1d)$, and $S^{^6\mathrm{Li}}_{^3\mathrm{He}t}(2s)$ were adjusted until the calculated cross sections yielded the best χ^2 fit to the 12- and 14-MeV data. Since the χ^2 criterion was not selective enough at the other energies, best qualitative visual fits were used instead. Table III shows the spectroscopic factors obtained, and Fig. 4 shows the resulting fits to the corresponding experimental angular distributions. Relative experimental errors are smaller than the data points, and the absolute normalization is good to 10%.

Fits could be obtained for the 12- to 18.5-MeV data with mean spectroscopic factors of:

$$S^{^6\mathrm{Li}}_{\alpha d}(2s)=0.69\,,$$

$$S^{^6\mathrm{Li}}_{\alpha d}(1d)=0.04\,,$$

$$S^{^6\mathrm{Li}}_{t^3\mathrm{He}}(2s)=0.44\,.$$

The value of 0.69 for the $2s$ relative state for the $\alpha+d$ system is large as expected and compares well with the value of 0.8 obtained by other methods.[28] The value of 0.44 for ^{3}He$+t$ clustering is somewhat smaller than the value of 0.69 obtained

TABLE III. Spectroscopic factors.

Energy (MeV)	^{6}Li $S_{\alpha d}(2s)$	^{6}Li $S_{\alpha d}(1d)$	^{6}Li $S_{^3\mathrm{He}t}(2s)$
8	1.03	0.012	0.57
10	0.76	0.045	0.36
12	0.76	0.045	0.36
14	0.62	0.038	0.50
16	0.66	0.032	0.45
18.5	0.66	0.032	0.45

by Young *et al.*[3] but is close to the value of 0.5 obtained by Kurdyumov, Neudatchin, and Smirnov.[29] In the analysis, the signs of the square roots of the spectroscopic factors were found to be the same.

The fits to the data at 8 and 10 MeV are not as good as those for the higher energies. This could be due to possible compound nuclear effects at the lower energies. The variation of the spectroscopic factors with energy may be due, in part, to energy dependence of the exit-channel optical-model parameters and nonlocal effects which were not included in the present formalism.

The relatively small spectroscopic factor obtained for $S_{\alpha d}^{^6Li}(1d)$ does not imply that inclusion of this term has little effect on the total cross section. As can be seen from Fig. 5, the $1d$ term plays a very important role in predicting the overall contribution to the total cross section, especially for the intermediate angles.

The present formalism does not include spin-orbit coupling in the distorted waves. However, the inclusion of spin-orbit effects in a direct pick-up zero-range calculation using DWUCK[30] does not significantly alter the calculated angular distribution of the $^6Li(p, ^3He)^4He$ reaction. Therefore, one might not expect spin-orbit effects to alter the results in the finite-range analysis.

Figure 6 illustrates the calculated angular distributions at 12 MeV with and without the exchange mode. By comparing the two curves, it is apparent that the exchange mode accounts for the sharp rise in the angular distribution at the background angles.

VII. DISCUSSION OF REACTION MECHANISMS

As demonstrated above, several mechanisms contribute to the total cross sections for the $^6Li(p, ^3He)$ reaction. The predicted cross sections associated with each mechanism used in fitting the 12-MeV data are illustrated in Fig. 3.

The total direct cross section associated with the $2s$ component of $\phi_{\alpha d}$ is compared with that

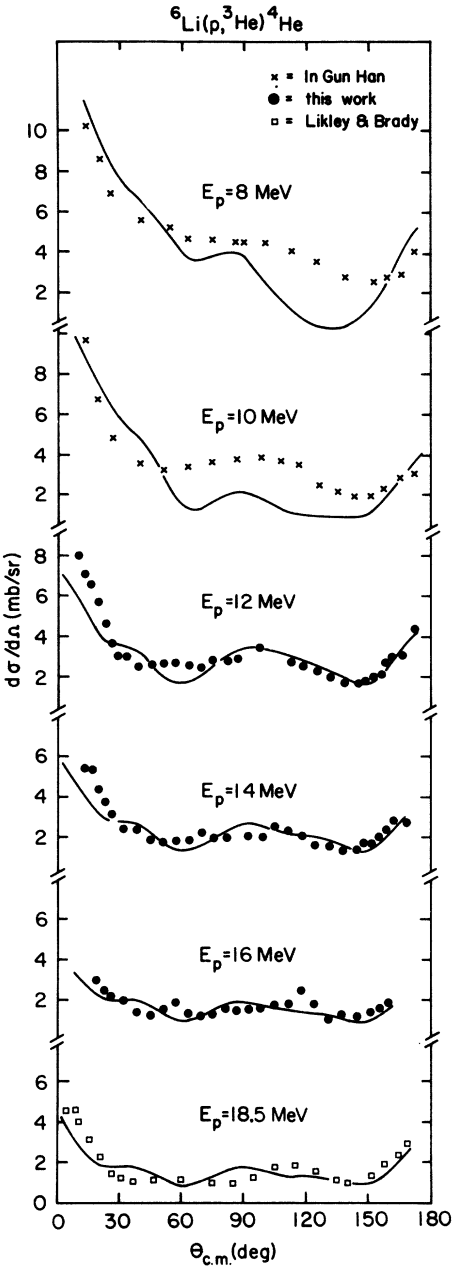

FIG. 4. Angular distributions of differential cross sections from the $^6Li(p, ^3He)^4He$ reaction at 8, 10, 12, 14, 16, and 18.5 MeV with relative experimental errors typically smaller than the data points.

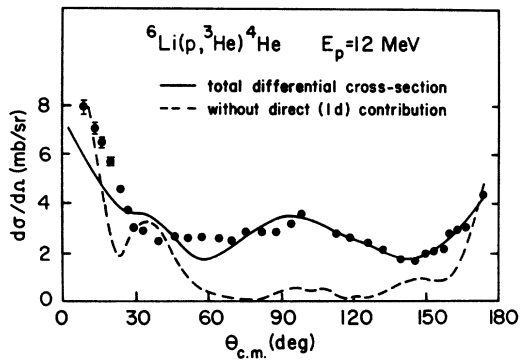

FIG. 5. A comparison of the experimental angular distribution from the $^6Li(p, ^3He)^4He$ reaction at 12 MeV with the total calculated cross section and the cross section obtained by omitting contributions corresponding to the $1d$ $\alpha + d$ target state.

predicted from the stripping potential V_{pd} (dashed curve) and the direct knockout potential $V_{p\alpha}$ (dotted curve). The pickup cross section which dominates the total cross section has sharp forward peaking, characteristic of stripping reactions associated with s-state form factors. The direct knockout contribution is also forward peaked but varies more smoothly with angle.

Because of the small separation energy between the α and d that form ^{6}Li, the $2s$ form factor is a rather extended system. Thus, the series generated by the overlap of this form factor with the partial wave functions required a fairly large number of terms before converging. Since the form factor changes sign, there will be considerable cancellation in that region where there is significant overlap with the partial waves. Such cancellation occurs for lower partial waves to the point at which the centrifugal barrier pushes the partial waves away from the first node. For this reason, the cross section associated with the $2s$ component of $\phi_{\alpha d}$ is less sensitive to choices of distorting potentials, i.e. contributions to the cross section occur at higher partial waves where the partial wave functions are approaching Coulomb radial functions.

The extracted reduced width for the $2s$ relative state of the $\alpha+d$ system is considerably larger than that for the $1d$ relative state. However, as can be seen by observing the top two solid curves of Fig. 3, the over-all contribution from the $1d$ form factor is the larger of the two. This effect, in part, is due to the cancellation associated with the $2s$ $\alpha+d$ form factor previosuly discussed which does not occur for the $1d$ form factor. A second reason has to do with the difference between angular momentum transfer for the two states. For the $2s$ state ($l=0$ transfer), there will be one radial integral for each outgoing partail wave, whereas for the $1d$ state ($l=2$ transfer), there will be three. In addition, one observes a relatively large direct knockout contribution for the $1d$ case (refer to Fig. 3) which was not the case when using the $2s$ form factor.

The difference between the two knockout contributions is related to the spatial region of the $V_{p\alpha}$ interaction (it occurs in the interior region of ^{6}Li) and the number of nodes of the form factor. Form factors which change sign, such as in the $2s$ case, will have a tendency to produce smaller contributions to direct knockout because of strong cancellation in the nuclear interior. The added importance of direct knockout for the $1d$ case serves to enhance the total cross section calculated from the form factor. As can be seen in Fig. 3, when direct pickup and direct knockout are coherently added, the resulting cross section is somewhat larger than that for either case. Thus, several factors come into play in enhancing the magnitude of the contribution to the cross section associated with the $1d$ component of the $\alpha+d$ relative state despite the relatively small value of $S_{\alpha d}^{^6\mathrm{Li}}(1d)$.

Figure 3 illustrates the cross sections associated with the various exchange mechanisms. The solid curve peaks sharply in the backward direction and along with the interference term (Fig. 7) accounts for most of the total cross section in the backward direction. The exchange cross section actually contributes little elsewhere. It is apparent from Fig. 6, which exhibits a fit to the cross section from only the direct mechanisms, that the cross sections at the backward angles can be described well by including the exchange mode but cannot with calculations that include only the direct mode.

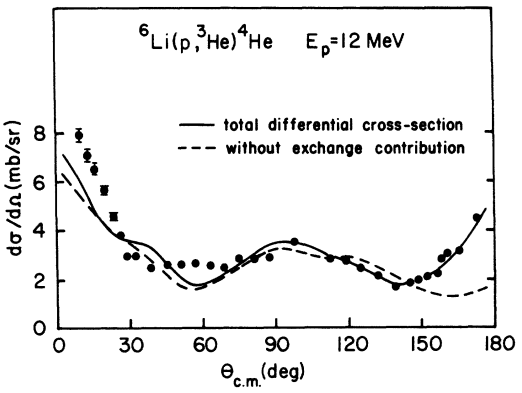

FIG. 6. A comparison of the experimental angular distribution from the ^{6}Li(p,^{3}He)^{4}He reaction at 12 MeV with the total calculated cross section and the cross section obtained by omitting exchange contributions corresponding to the $2s$ ^{3}He$+t$ target state.

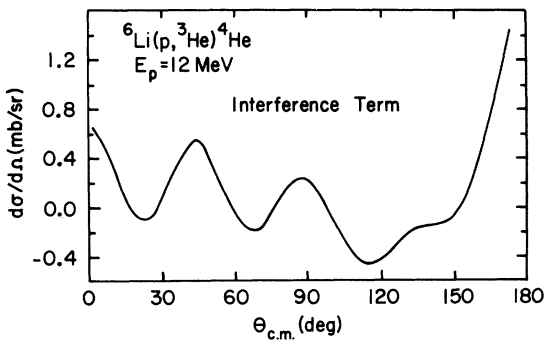

FIG. 7. The interference between the direct and exchange modes for the ^{6}Li(p,^{3}He)^{4}He reaction at 12 MeV indicated as positive when constructive and negative when destructive.

It is interesting to note that though the exchange pickup and knockout potentials are equal except for the Coulomb interaction ($V_{ph} = V_{p^3He}$), the magnitude of the pickup contribution is somewhat larger than that of knockout, and the shapes are similar except for extreme forward angles. This is true because the pickup term has the same coordinates as that of the $^3He + t$ form factor, i.e. it is a diagonal term, while the knockout term is off-diagonal.

Figure 7 illustrates the importance of the interference term in this analysis. It is apparent from the figure that the interference term can be either constructive or destructive depending on the angle. By comparing the magnitude of the interference term to the cross section calculated from total exchange, it can be seen that it is as important as the exchange term alone. Thus, if it were ignored in this calculation, the value of $S^{^6Li}_{^3He\,t}$ would have been a factor of 2 too large.

VIII. CONCLUSION

In order to adequately describe angular distributions of differential cross sections from the $^6Li(p, ^3He)^4He$ reaction at 8, 10, 12, 14, 16, and 18.5 MeV, it was necessary to apply a finite-range two-mode multi-interaction DWBA analysis. Exchange effects, attributable to considerable $^3He + t$ clustering in the target state, accounted for the sharp backward-angle peaking observed in the data. A relatively small value for $S^{^6Li}_{\alpha d}(1d)$ associated with the $1d$ relative state of the $\alpha + d$ system produced a marked effect on the calculated angular distribution. Possible d-state components of the $^3He + t$ and $d + p$ relative states discussed in Sec. IV were expected to be less important than in the $\alpha + d$ system and were not included in this analysis.

ACKNOWLEDGMENTS

The authors would like to thank the Florida State University tandem accelerator group and maintenance personnel for help with the FN tandem. It is out pleasure to thank Y. C. Tang of the University of Minnesota for providing some of the ^6Li wave functions, and In Gun Han and N. P. Heydenburg for allowing us to use their $^6Li(p, ^3He)^4He$ data. We also express our gratitude to R. J. Philpott and D. Robson for enlightening discussions.

---

*Research supported in part by the National Science Foundation, Grant Nos. NSF-GJ-367, GP-15855, GU-2612, and NSF-GP-25974.

[1]K. Wildermuth and W. M. McClure, *Springer Tracts in Modern Physics*, edited by G. Höhler (Springer, New York, 1966), Vol. 41; D. R. Thompson and Y. C. Tang, Phys. Rev. **179**, 971 (1969); S. Fautoni and S. Rosati, Nucl. Phys. **A151**, 317 (1970); G. C. Phillips and T. A. Tombrello, Nucl. Phys. **19**, 555 (1960).

[2]P. Goldhammer, Rev. Mod. Phys. **35**, 40 (1963).

[3]S. L. Blatt, A. M. Young, S. C. Ling, K. J. Moon, and C. D. Porterfield, Phys. Rev. **176**, 1147 (1968); A. M. Young, S. L. Blatt, and R. G. Seyler, Phys. Rev. Lett. **25**, 1746 (1970).

[4]D. Bachelier, M. Bernos, C. Detraz, P. Radvanyi, and M. Roy, Phys. Lett. **26B**, 283 (1968).

[5]J. M. Lambert, R. J. Kane, P. A. Treado, L. A. Beach, E. L. Peterson, and R. B. Theus, Phys. Rev. C **4**, 2010 (1971).

[6]R. D. Amado and J. V. Noble, Phys. Rev. C **3**, 2494 (1971).

[7]L. Madansky and G. E. Owens, Phys. Rev. **99**, 1608 (1955); S. Edwards, Nucl. Phys. **47**, 652 (1963).

[8]T. L. Talley, Ph. D. dissertation, The Florida State University, 1968 (unpublished).

[9]H. G. Bingham, A. R. Zander, K. W. Kemper, and N. R. Fletcher, Nucl. Phys. **A173**, 265 (1971).

[10]S. Edwards, D. Robson, T. L. Talley, W. J. Thompson, and M. F. Werby, Phys. Rev. C (to be published).

[11]Y. C. Tang, private communication.

[12]D. Robson, Notes on Two-Mode Stripping Theory, The Florida State University, 1963 (unpublished).

[13]M. F. Werby, Ph.D. dissertation, The Florida State University, 1971 (unpublished).

[14]R. Jastrow, Phys. Rev. **98**, 1479 (1955).

[15]J. N. Pappademos, Nucl. Phys. **42**, 122 (1963).

[16]Hr. Collard, L. R. B. Elton, and R. Hofstadter, in *Handbuch der Physik*, edited by H. Schopper (Springer-Verlag, Berlin, 1967), Vol. 2.

[17]S. Gartenhaus, Phys. Rev. **100**, 900 (1956); M. J. Morovcsik, Nucl. Phys. **7**, 113 (1958).

[18]L. P. Kok and A. S. Rinot, Nucl. Phys. **A156**, 593 (1970).

[19]P. W. Keaton, E. Aufdembrink, and L. R. Veeser, Los Alamos Scientific Laboratory Report No, LA-4379-MS, 1970 (unpublished).

[20]S. Sack, L. C. Biedenharn, and G. Breit, Phys. Rev. **93**, 321 (1954).

[21]B. A. Watson, P. P. Singh, and R. E. Segel, Phys. Rev. **182**, 977 (1969).

[22]L. Rosen, J. G. Beery, and A. S. Goldhaber, Ann. Phys. (N.Y.) **34**, 96 (1965).

[23]F. Dunnil, T. J. Gray, H. T. Fortune, and N. R. Fletcher, Nucl. Phys. **A93**, 201 (1967).

[24]E. J. Squires, A. E. Forest, and P. G. Hodgson, Nucl. Phys. **42**, 490 (1963).

[25]G. R. Satchler, L. W. Owen, A. J. Elwyn, G. L. Morgan, and R. L. Walter, Nucl. Phys. **A112**, 1 (1968).

[26]In Gun Han and N. P. Heydenburg, private communication.

[27]J. G. Likely and F. P. Brady, Phys. Rev. **104**, 118 (1956).

[28]J. C. Alder, W. Dollhopf, W. Kossler, C. F. Perdrisat, W. K. Roberts, P. Kitching, G. A. Moss, W. C. Olsen, and J. R. Priest, Phys. Rev. C **6**, 18 (1972).

[29]I. V. Kurdyumov, V. G. Neudatchin, and Yu F. Smirnov, Phys. Lett. **31B**, 426 (1970).

[30]P. D. Kunz, private communication.